Semi-calibrated Near Field Photometric Stereo Supplementary Material

Fotios Logothetis[1], Roberto Mecca*[1,2], Roberto Cipolla[1]
{fl302, rm822, rc10001}@cam.ac.uk
[1]Department of Engineering, University of Cambridge, United Kingdom
[2]Department of Mathematics, University of Bologna, Italy

1. Synthetic Datasets

In this section we presented all 24 images for our three synthetic datasets, namely "fully orthographic" (Figure 1), near field diffuse reflection (Figure 2) and near field Cook & Torrance (Figure 3). We used the following formulation of the Cook and Torrance irradiance equation:

$$i = a\rho\left(\rho_s \frac{fdg}{\pi(\overline{\mathbf{N}}\cdot\overline{\mathbf{L}})(\overline{\mathbf{N}}\cdot\overline{\mathbf{V}})} + \rho_d(\overline{\mathbf{N}}\cdot\overline{\mathbf{L}})\right) \quad (1)$$

where

$$\mathbf{H} = \overline{\mathbf{L}} + \overline{\mathbf{V}} \quad (2)$$

$$f = f_0 + (1-f_0)(1-(\overline{\mathbf{V}}\cdot\overline{\mathbf{H}}))^5 \quad (3)$$

$$d = \frac{1}{\pi r^2(\overline{\mathbf{N}}\cdot\overline{\mathbf{H}})^4} e^{\left(\frac{(\overline{\mathbf{N}}\cdot\overline{\mathbf{H}})^2-1}{r^2(\overline{\mathbf{N}}\cdot\overline{\mathbf{H}})^2}\right)} \quad (4)$$

$$g = \min\left(1, \frac{2(\overline{\mathbf{N}}\cdot\overline{\mathbf{H}})(\overline{\mathbf{N}}\cdot\overline{\mathbf{V}})}{(\overline{\mathbf{V}}\cdot\overline{\mathbf{H}})}, \frac{2(\overline{\mathbf{N}}\cdot\overline{\mathbf{H}})(\overline{\mathbf{N}}\cdot\overline{\mathbf{L}})}{(\overline{\mathbf{L}}\cdot\overline{\mathbf{H}})}\right) \quad (5)$$

For the constants, we used the following values: $f_0 = 0.75$, $r = 0.45$ $\rho_s = 0.75$ and $\rho_d = 0.25$.

2. Real Data

2.1. Real Data sequences

In this section we present the complete sequence of images used for real data experiments. These can be seen in Figures 4, 5 and 6. These color images are generated by noting position of each pixel on the Bayer filter of our camera, thus no white balancing is enforced. The same coloring technique is used for displaying RGB albedo. It should be emphasized that at the pixel level, we just have scalar intensity values and scalar albedos and these scalar values are the inputs and outputs of our algorithm. Uncolored raw data can be seen in Figure 7(a).

*Roberto Mecca is a Marie Curie Fellow of the Istituto Nazionale di Alta Matematica, Italy.

2.2. Intermediate results

In this section, we show a few illustrative examples of the intermediate outputs that are computed by our method. These include shadow maps, light attenuation maps and shininess parameter maps.

It is important to stretch that our shadow map detection algorithm is not guaranteed to find all shadows, as they may be caused by objects outside the field of view of the camera (such as the left hand of the Armadillo in the last two images of Figure 6). However, regions marked as shadows are almost certainly true positives and should definitely be ignored for the rest of the calculations.

We also present some calculated attenuation maps in Figure 7(c). Attenuation map values in regions found in or surrounding shadows are useless. Indeed, these pixels are ignored for further calculations (unless a new estimate of the geometry in a future iteration shows that these pixels are not in shadow). As the calculated attenuation maps (Figure 7(c)) are not very meaningful on their own, we present for comparison the attenuation maps that one would get assuming point light source, shown in Figure 7(d). These are not used by our method but provide a useful insight on the limitation of the point light source assumption. The calculated attenuation maps are much more detailed and thus allow for higher reconstruction quality.

Finally, we include for completeness shininess parameter maps in Figure 7(e). The non-physical derivation of the irradiance equation used in the paper does not allow to the shininess parameter to provide precise hint regarding the material. In fact, perfect white means purely diffuse reflection but even at 0.95% whiteness, there is a non-negligible divergence from such reflection as the weighted light vector $\mathbf{W}$ diverges away from the light vector $\mathbf{L}$.

Figure 1. Synthetic, “fully orthographic” data.

Figure 2. Synthetic, near field, diffuse reflectance data.

Figure 3. Synthetic, near field, Cook & Torrance reflectance data.

Figure 4. Complete “baseball player figurine” sequence.

Figure 5. Complete “hand” sequence.

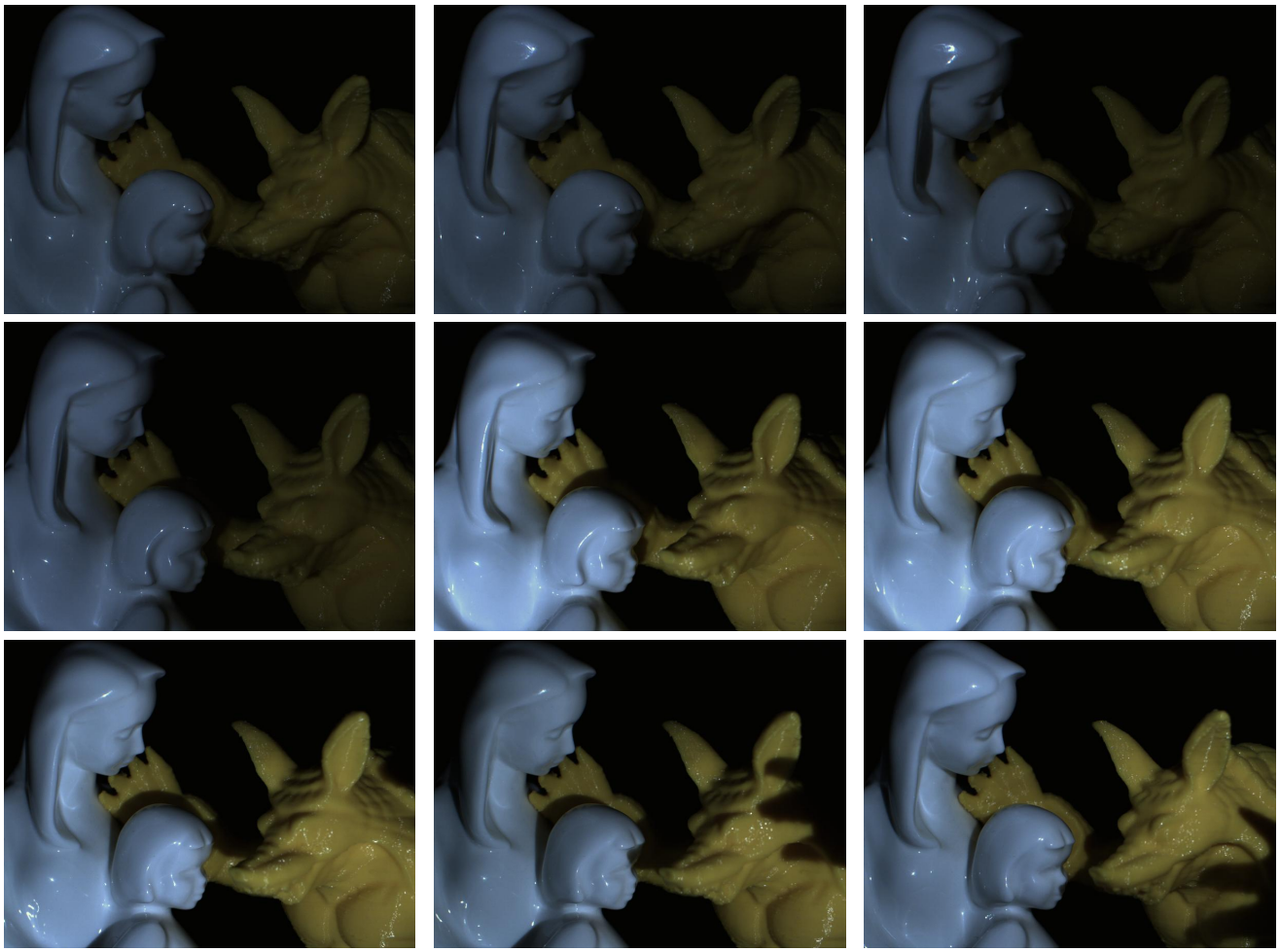

Figure 6. Complete “Statue & Armadillo” sequence.

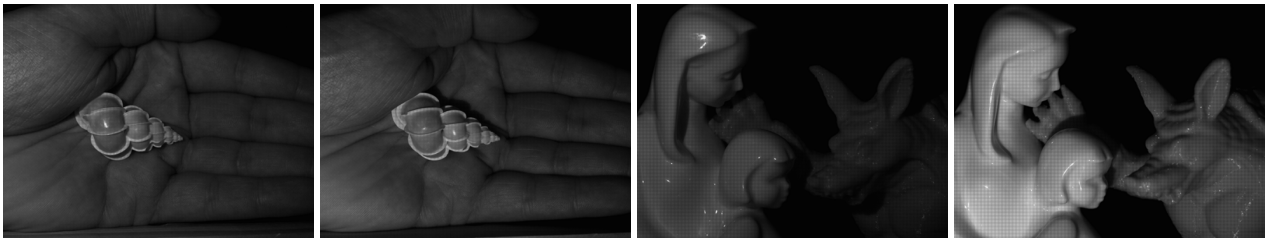

(a) Raw Data

(b) Computed shadow maps

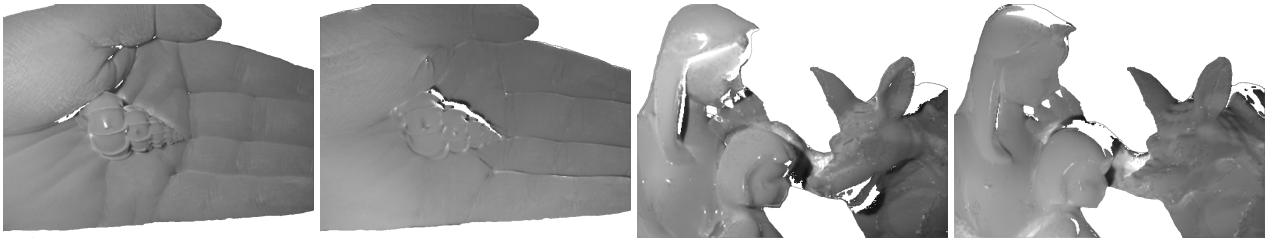

(c) Calculated attenuation maps (shaded regions have meaningless value).

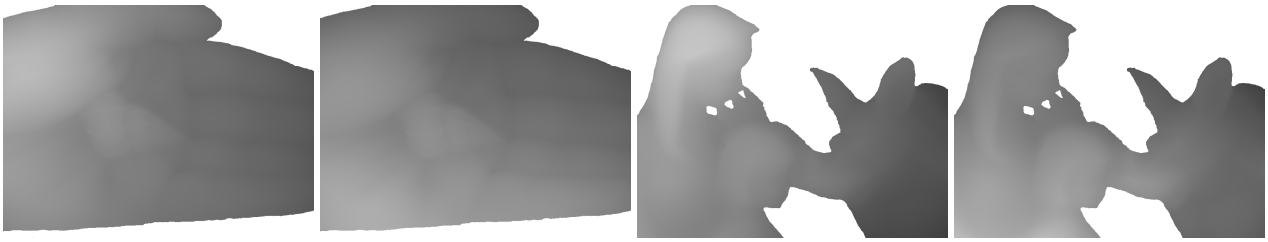

(d) Attenuation maps assuming point source (not used for reconstructions).

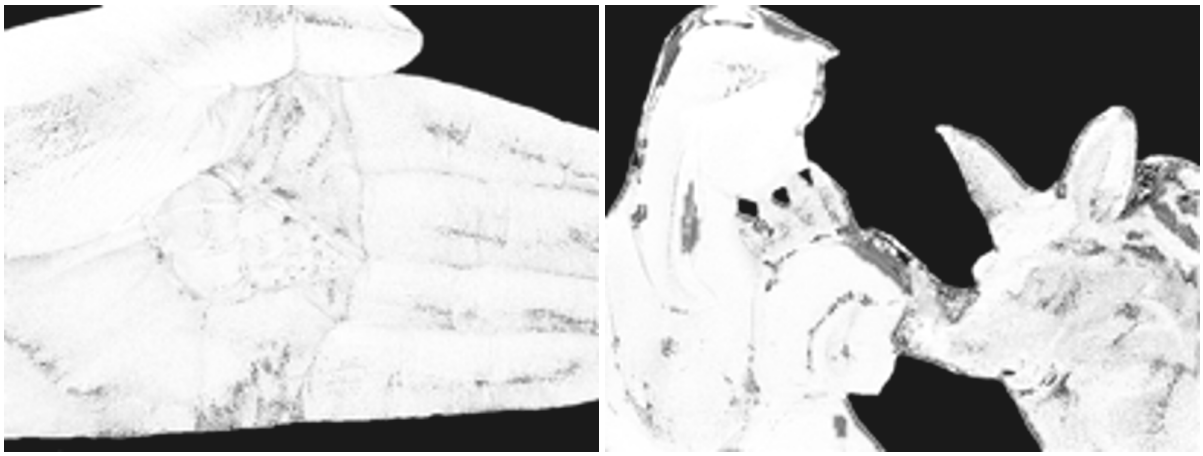

(e) Shininess parameter C map.

Figure 7. Illustative samples from intermediate results of our algorithm.